JACS
JOURNAL OF THE AMERICAN CHEMICAL SOCIETY

Article

pubs.acs.org/JACS

Mechanism of Tau-Promoted Microtubule Assembly As Probed by NMR Spectroscopy

Benoît Gigant,[†,+] Isabelle Landrieu,[‡,§,+] Caroline Fauquant,[†] Pascale Barbier,[∥] Isabelle Huvent,[‡] Jean-Michel Wieruszeski,[‡,⊥] Marcel Knossow,[†] and Guy Lippens*[,‡]

[†]Laboratoire d'Enzymologie et Biochimie Structurales, Centre de Recherche de Gif, Centre National de la Recherche Scientifique, 91198 Gif sur Yvette, France

[‡]Unité de Glycobiologie Structurale et Fonctionnelle, CNRS UMR8576, Université de Lille1, Centre National de la Recherche Scientifique, 59655 Villeneuve d'Ascq, France

[§]Institut de Recherche Interdisciplinaire, CNRS USR 3078, Centre National de la Recherche Scientifique, 59655 Villeneuve d'Ascq, France

[∥]Aix-Marseille Université, CRO2 INSERM UMR_S 991, 13385 Marseille cedex5, France

Supporting Information

ABSTRACT: Determining the molecular mechanism of the neuronal Tau protein in the tubulin heterodimer assembly has been a challenge owing to the dynamic character of the complex and the large size of microtubules. We use here defined constructs comprising one or two tubulin heterodimers to characterize their association with a functional fragment of Tau, named TauF4. TauF4 binds with high affinities to the tubulin heterodimer complexes, but NMR spectroscopy shows that it remains highly dynamic, partly because of the interaction with the acidic C-terminal tails of the tubulin monomers. When bound to a single tubulin heterodimer, TauF4 is characterized by an overhanging peptide corresponding to the first of the four microtubule binding repeats of Tau. This peptide becomes immobilized in the complex with two longitudinally associated tubulin heterodimers. The longitudinal associations are favored by the fragment and contribute to Tau's functional role in microtubule assembly.

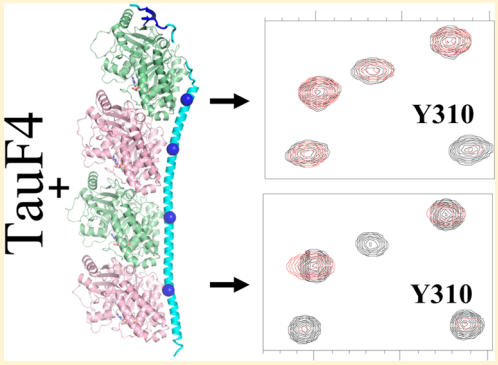

INTRODUCTION

Tau is a microtubule-associated protein that in vivo and in vitro promotes the assembly of microtubules from a pool of soluble α/β tubulin heterodimers.[1,2] Electron and video-microscopy measurements on both bulk[3] and individual[4] microtubules indicated that its main effect is to protect against depolymerization by lowering the dissociation of tubulin heterodimers at both (+) and (−) ends of the microtubule, resulting in an increased growth rate and decreased catastrophe frequency.

The mechanistic details of how Tau promotes tubulin heterodimer polymerization have proven elusive. A first body of research has focused on the identification of Tau residues involved in the interaction with stabilized microtubules. On the basis of work with Tau fragments, multiple weak interactions of the protein with the microtubule surface have been suggested, especially mediated by the four repeating peptides in the C-terminal half of the protein that thereby became known as the microtubule binding repeats R1−R4 (MTBRs; see Figure 1 for the primary structure and definition of peptides).[5] Later, a concerted binding of the MTBRs and the flanking regions was proposed.[6] The requirements to be fulfilled by Tau sequence elements to obtain a functional and tight complex with microtubules have been characterized further, identifying, in particular, hotspots[7] and suggesting that intramolecular interactions between the proline rich region (PRR) upstream of the MTBRs and the repeats might be needed.[8] In a second approach, the location of Tau binding sites on microtubules was investigated. Alignment of Tau on the outer surface of taxol-stabilized microtubules, both along and across protofilaments, has been inferred from cryoelectron microscopy images,[9,10] whereas atomic force microscopy[11] and isothermal titration calorimetry[12] located it predominantly along the protofilaments. To make the situation even more complicated, when Tau is coassembled with tubulin heterodimers into a Tau:tubulin copolymer rather than fixed to a preassembled microtubule, additional interaction sites might exist.[13] For the latter case of coassembly, a binding site of Tau close to the taxol binding site of β-tubulin, at the lumen of the microtubules, has been suggested.[14] Occupancy of the taxane pocket on β-tubulin stabilizes the lateral contacts between protofilaments.[15] Tau isoform-specific regulation of the number of protofilaments in microtubules[16] could involve a similar interaction. Nevertheless, the precise localization of Tau has been hampered in particular

Received: May 15, 2014
Published: August 27, 2014

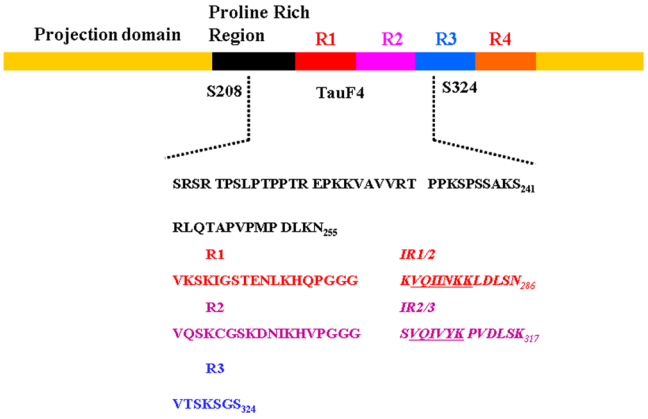

Figure 1. Domain organization of Tau441 and sequence of the TauF4 fragment. Numbering is according to the 441 amino acid long adult isoform. The repeat and inter-repeat regions are as defined by Lee et al.[24,25] The PHF6 (V306−K311) and PHF6* (V275−K281) peptides, thought to be the nuclei for the aggregation of Tau into fibers,[26,27] are underlined.

by its migration on the microtubule surface, as was suggested[5] early on and recently observed by single molecule fluorescence.[17]

Because of the lack of detailed structural data, open questions remain about the functional interaction of Tau with microtubules. The first question concerns the molecular mechanism by which Tau promotes the first steps of assembly of individual tubulin heterodimers into protofilaments and/or microtubules. This question concerns the interaction of Tau with a single tubulin heterodimer and how this interaction lowers the critical concentration for microtubule assembly. Second, how does it protect microtubules from depolymerization: what are the regions of Tau involved and what are their roles? A third question relates to the structure of Tau when bound to tubulin heterodimers, protofilaments, or microtubules. Tau is an intrinsically unstructured protein (IUP) when isolated in solution.[18−22] Whereas many IUPs have been shown to adopt a well-defined fold upon binding to their cognate partner,[23] such might not be the case for Tau, but direct evidence is lacking. A structural characterization of Tau when bound to tubulin or to tubulin assemblies would help to clarify this issue.

Here we study a fragment of Tau, TauF4 (Figure 1), that both binds tightly to MTs and favors their assembly, thus recapitulating two important characteristics of the interaction of the whole protein with tubulin heterodimers.[28] We first show that this fragment favors the longitudinal interaction of individual tubulin heterodimers and thereby plays a positive role in the construction of protofilaments. Then using NMR spectroscopy we exploit the availability of soluble tubulin complexes comprising a single or two heterodimers to detail how this functional fragment of Tau binds to the tubulin surface. We find that the Tau fragment largely binds without adopting a regular secondary structure and that, despite the high affinity of the partners, molecular mobility remains a defining factor of the complexes tested. Finally, our structural model provides a framework to study the physiological role of Tau phosphorylation.

EXPERIMENTAL SECTION

Effect of TauF4 on the GTPase Activity of Tubulin−Colchicine. The tubulin−colchicine complex was prepared as described previously.[29] The GTPase measurements were performed at a 10 μM tubulin−colchicine concentration in 80 mM PIPES-K, pH 6.8, 2 mM $MgCl_2$, 0.5 mM EGTA, 150 μM [γ-^{32}P]GTP, in the presence of TauF4 at variable concentrations.

Sedimentation Assay. A constant concentration of 10 μM tubulin heterodimer−colchicine (Tc) was incubated with increasing concentrations of TauF4, in a 80 mM PIPES-based buffer, 1 mM $MgCl_2$, 0.5 mM EGTA, 150 μM GTP. Samples were centrifuged at high speed (315 000g, 34 °C) for 10 min after 20 min of incubation at 37 °C, or at low speed (20 000g, 34 °C) for 15 min after 45 min incubation at 37 °C. Pellets and supernatants were collected and analyzed by SDS-PAGE.

Electron Microscopy. Samples were prepared at 20 °C with 5 μM tubulin heterodimers alone and with different TauF4 concentrations (from 2 to 18 μM) in 20 mM phosphate buffer, pH 6.5, 10 μM GTP. Samples were adsorbed onto Formvar carbon-coated copper grids, stained with 2% (w/v) uranyl acetate, and blotted to dryness. Grids were observed using a JEOL JEM-1400 electron microscope operated at 80 kV.

Sample Preparation. The complex of tubulin with an SLD-based domain (SLD = stathmin-like domain) that sequesters one tubulin,[30] complexes of tubulin and of subtilisin-digested tubulin with $RB3_{SLD}$,[31,32] and the Ncap-tubulin[33] complex were prepared as described. The TauF4 fragment was prepared as a triply labeled protein (^{2}H, ^{13}C, ^{15}N) by overexpression in a deuterated culture medium. Further details are given in the Supporting Information.

TauF4 Interaction Assay with the Different Tubulin Heterodimer Complexes. A mutant of TauF4, in which one of the cysteine residues (at position 322, residue numbering as in the longest isoform of human Tau) had been mutated to a serine, was obtained by standard molecular biology techniques, purified as TauF4, reduced with dithiothreitol, and then reacted with acrylodan. This protein was used in a titration experiment against the different tubulin heterodimer complexes as described in the Supporting Information.

NMR Spectroscopy. NMR spectra were acquired on a Bruker 800 MHz Avance II instrument with a triple resonance probe head, or on a 900 MHz Avance III instrument, equipped with a cryogenically cooled triple resonance probe head. Details of the sample conditions and spectral acquisition parameters are given in the Supporting Information.

RESULTS

TauF4 Promotes the Longitudinal Association of Tubulin Heterodimers. In the microtubule, the tubulin heterodimer interacts longitudinally with its nearest neighbors along protofilaments. Stabilizing these interactions is therefore one way to favor microtubule assembly. To verify whether TauF4 may use such a mechanism, we recorded its effect on the GTPase activity of the tubulin heterodimer−colchicine complex, which has been shown to depend on such longitudinal associations.[34,35] We indeed observed an increased GTP hydrolysis rate upon addition of TauF4 to a fixed concentration of tubulin heterodimer−colchicine (Figure 2a). As expected, this GTPase activity is inhibited by vinblastine, a compound that binds at the longitudinal interface between two tubulin heterodimers.[36]

To investigate whether these longitudinal interactions lead to protofilaments, we performed an assembly experiment of tubulin heterodimers. Whereas a sample of 10 μM of tubulin heterodimer−colchicine forms oligomers that can be visualized by centrifugation at high speed (315 000g) but not at low speed (20 000g), increasing amounts of TauF4 stabilize the oligomers to such an extent that at equimolar concentrations of TauF4 and tubulin heterodimer−colchicine, a major part of the tubulin heterodimer−colchicine is found in the pellet even when centrifuging the sample at low speed (Figure 2b). To visualize the resulting oligomers, we incubated a sample with TauF4 and tubulin heterodimers at 20 °C, a temperature whereby no full

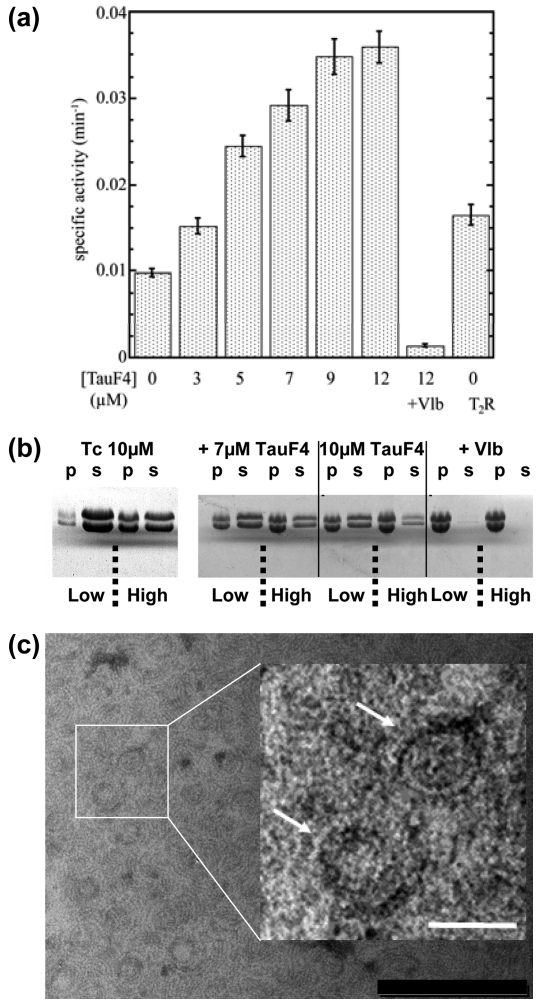

Figure 2. TauF4 promotes the longitudinal assembly of tubulin heterodimers. (a) TauF4-enhanced tubulin–colchicine GTPase activity. The GTPase activity of tubulin–colchicine (10 μM) was recorded in the presence of increasing TauF4 concentrations. The catalytic activity is inhibited to close to background level by vinblastine (Vlb, 50 μM added). For comparison, the GTPase in the presence of $RB3_{SLD}$ (T_2R) was also measured. (b) TauF4 promotes oligomer formation of tubulin heterodimers in the presence of colchicine. In the presence of TauF4, these oligomers can be found in the pellet (p) even when centrifuging at low speed, whereas without TauF4, Tc is mainly found in the supernatant (s). (c) Electron micrograph of TauF4-induced tubulin ring structures. Scale bar (black) = 200 nm, scale bar (white) of insert = 50 nm.

microtubules should form. Observation of the sample by electron microscopy showed circular polymers of diameter 42 ± 4 nm, usually called tubulin rings, that resemble the curved protofilaments[37] (Figure 2c). Without TauF4, the same tubulin heterodimers do not induce any ring structures (Figure S1, Supporting Information). Overall, these results indicate that TauF4 favors the longitudinal association of tubulin heterodimers.

TauF4 Binds Tightly to Nonpolymerizable Tubulin Heterodimers but Remains Dynamic in the Complex. To study the Tau–tubulin interaction at the molecular level, we sought to use NMR spectroscopy, a method that has previously given access to structural details of flexible parts in a large macromolecular complex[38] and is well suited to deal with dynamical systems. Stabilized microtubules are however too large for the technique. Indeed, whereas solution NMR of Tau-decorated microtubules previously allowed the observation of the N-terminal projection domain and C-terminus of Tau, residues in the direct interaction region could only be identified by broadening or lack of signal.[39,40] Free tubulin heterodimers are not a good candidate either, because stoichiometric amounts of Tau lower the critical concentration for MT assembly to submicromolar values, below the minimal concentration of tens of micromolar required for solution NMR. We therefore turned to tubulin heterodimer complexes that are prevented from assembling into MTs. We have previously shown[28] that a fragment of Tau devoid of the projection domain binds to tubulin embedded in T_2R, the complex composed of two tubulin heterodimers sequestered by the stathmin-like domain of the RB3 protein ($RB3_{SLD}$).[41,29] Exploiting the FRET signal between the tubulin tryptophans and acrylodan-labeled TauF4, we find that under NMR conditions, the dissociation constant (K_D) of TauF4 from T_2R is lower than 1 nM (Figure 3). Thus, we expect a complex that is stable on the NMR time scale.

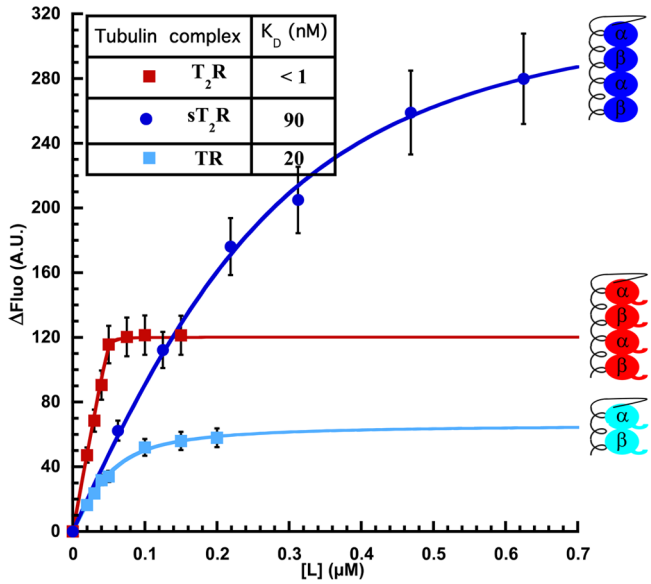

Figure 3. The affinity of TauF4 for different complexes of tubulin heterodimers with stathmin-like-based proteins, monitored by fluorescence spectroscopy.

The NMR spectrum of TauF4 is considerably simpler than that of full-length Tau and should hence give easier access to structural parameters.[42] We have ^{15}N-, ^{13}C-, ^{2}D-labeled TauF4 for the NMR spectroscopy study of its interaction with T_2R. Despite the absence of deuteration of T_2R and the more than 200 kDa molecular weight of the resulting complex, the resulting transverse relaxation optimized spectroscopy (TROSY) spectrum was of good quality and allowed the recording of a 3D TROSY-HNCACB experiment for the assignment. Significant chemical shift differences, similar in size and direction to those observed upon binding of Tau to heparin,[43] were observed for most amide cross-peaks in the PRR (Figures 4, 5, and S2, Supporting Information). The most significant shift was observed for resonances in the N-terminal part of the PRR (for examples see Figure S2 and Table S1, Supporting Information). However, Cα and Cβ chemical shift values for residues in the PRR did not vary significantly

dx.doi.org/10.1021/ja504864m | J. Am. Chem. Soc. 2014, 136, 12615–12623

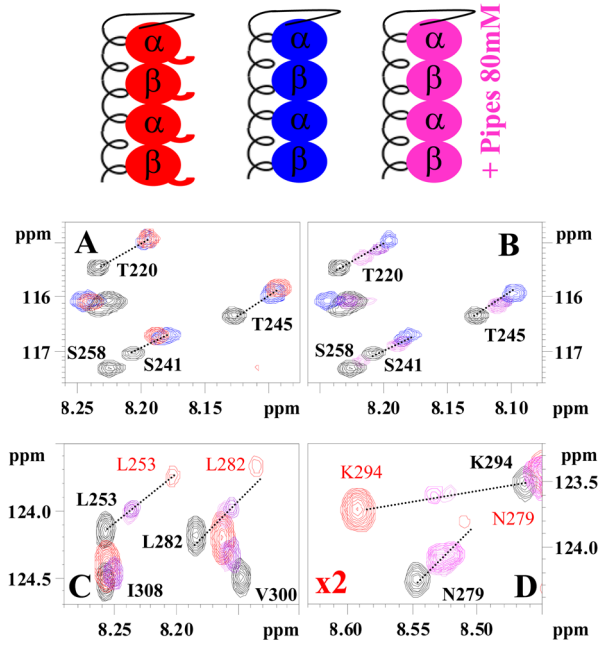

Figure 4. The role of the C-terminal Glu-rich tubulin peptides in the anchoring of TauF4. Schematic drawing of the T_2R and sT_2R complexes used, in colors that correspond to the NMR spectra. (A) Similar shifts for resonances of TauF4 (black when isolated) are observed when in the complex with sT_2R (blue) compared to T_2R (red). (B) Titration behavior for the complex of TauF4 with sT_2R in 80 mM PIPES-K buffer. Spectra with a 0.8:1 and 0.3:1 ratio of TauF4:sT_2R in 80 mM PIPES-K buffer are shown in pink and violet, respectively. The spectrum in blue is the TauF4:sT_2R spectrum in 15 mM PIPES-K buffer. Residues in the R1 repeat (as here Ser258) lose their resonances after the first titration point. (C) Although the peaks of reduced intensity in the TauF4:T_2R spectrum disappear in the TauF4:sT_2R spectrum at 15 mM PIPES-K buffer, they are visible in the initial steps of the titration experiment in 80 mM PIPES-K, and indicate the direction for the final peak in the TauF4:T_2R spectrum. (D) Idem as C, but with ratios 0.8:1 and 0.5:1 for TauF4:sT_2R in 80 mM PIPES. The red TauF4:T_2R spectrum is contoured at 2× lower levels.

between the free TauF4 fragment and TauF4 in its complex with T_2R (Figure S2, Table S3, Supporting Information), thereby arguing against the adoption of a stable secondary structure for the PRR region.

The second contiguous peptide we could unambiguously assign on the basis of the Cα/Cβ carbon frequencies was the IR2/3 (IR = inter-repeat) region and the part of R3 present in TauF4 (Figure 1). Resonance peaks shift less than those corresponding to residues in the PRR and do not show a consistent upfield pattern (Figure S2, Supporting Information). However, even for the PHF6 peptide (PHF = paired helical filament) thought to be a nucleus for aggregation[26] (Figure 1), ^{13}C chemical shift values do not vary significantly between the free and bound state (Figure S2, Supporting Information). The regular β strand adopted by this peptide in its amyloid form[44,45] hence does not reflect its tubulin-bound conformation.

Assignment of residues in the R1 and R2 repeats and inter-repeat region proved more difficult. Indeed, the last residue we could connect to its upstream neighbor on the basis of its Cα/Cβ signals was Val248, before the start of the first repeat. Intensity after this residue severely dropped, and even for an isolated correlation peak such as that for Gly261, we could not find a plausible counterpart in the spectrum of the bound

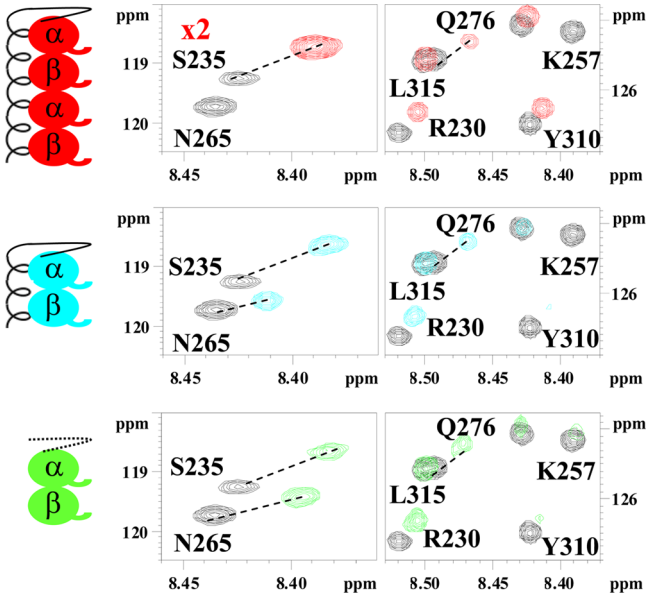

Figure 5. Comparison of the TauF4 interaction with different tubulin complexes. Spectra of TauF4:T_2R (top, red), of TauF4:TR (middle, light blue), and of TauF4:Ncap-tubulin (bottom, light green) show the presence of signals for Asn265 in the latter two spectra, whereas this resonance is completely absent from the TauF4:T_2R spectrum. In contrast, the intense peak of Tyr310 in the TauF4:T_2R spectrum is severely reduced in the spectra of TauF4 with a single tubulin heterodimer. The red TauF4:T_2R spectrum in the panel with Ser235 is contoured at 2× lower levels to show the absence of the Asn265 cross-peak. A schematic representation of the different soluble tubulin constructs is given on the left of each spectrum.

TauF4. However, for a couple of isolated peaks such as those for Gln276 in IR1/2 or Val300 in R2 (Figure 5, top, and Figure S2, Supporting Information), magnetization transfer in the TROSY-HNCACB spectrum did occur and points to spots of local mobility. Even for these residues, the carbon frequencies did not appreciably vary between free and bound form. A number of other weaker peaks are observed in the TROSY spectrum but could only be tentatively assigned to residues in R1−R2 on the basis of proximity to peaks in the spectrum of TauF4.

Despite the important contribution of the PRR to the overall high affinity of the complex,[28] these results highlight its remaining dynamical character when bound to T_2R. The same is true for the C-terminal part of TauF4, comprising the IR2/3 and R3 peptides. The disappearing signals for most residues in the internal R1 and R2 repeats hinder atomic characterization at this stage.

Part of the TauF4 Dynamicity Is Conferred by Its Interaction with the Tubulin C-Terminal Tails. A dominant role for the tubulin C-terminal tails in mediating the interaction with Tau has been proposed.[46,47] One characteristic of these C-terminal tails is that they are enriched in acidic residues and highly mobile. Indeed, the C-terminal tail could be traced in electron density maps of tubulin structures only in the α subunit and when in complex with tubulin−tyrosine ligase, an enzyme that specifically interacts with this part of tubulin.[48] To investigate the role of tubulin C-terminal tails in Tau binding, we prepared a T_2R construct in which the tubulin tails have been cleaved by subtilisin (sT_2R).[32] When measuring the affinity of TauF4 for sT_2R in a FRET experiment, the association constant indeed decreases by 2

dx.doi.org/10.1021/ja504864m | J. Am. Chem. Soc. 2014, 136, 12615−12623

orders of magnitude (Figure 3), confirming a role for these flexible tails in the anchoring of Tau.

Despite this drop in affinity, the TROSY spectrum of the TauF4 fragment in complex with sT_2R shows that the ^{1}H, ^{15}N chemical shift differences for residues in the PRR are only marginally different from those observed in the complex with T_2R (Figure 4). The surface of the T_2R complex, even when calculated from the structure without the negatively charged C-terminal tails, remains very electronegative (Figure S3, Supporting Information). This negatively charged surface rather than specific hydrogen bonding between amide functions of TauF4 and acidic side chains of the tubulin tails in TauF4:T_2R hence can explain the observed shifts.[49] The resonance intensity of some selected residues in this region, such as Leu215, already weak in the spectrum of TauF4:T_2R, further decreased when in complex with sT_2R (Table S2, Supporting Information). A small but observable effect of the removal of the tubulin tails on the peak position was detected when approaching the R1 repeat (e.g., S241 and Thr245 in Figure 4) and was accompanied by an earlier drop in intensity than in the complex with T_2R. The resonance of Val248, for example, hardly reaches above noise level in the TauF4:sT_2R spectrum (Figure S4, Supporting Information). This signal decrease, indicative of loss in mobility, further extends in the repeats region, as peaks such as those of Gly271 and Gln276 and many of the other weak peaks tentatively assigned to the R1−R2 region in the TauF4:T_2R spectrum completely disappear after removal of the tubulin C-terminal tails (Figure S4, Supporting Information). The chemical shift values of resonances corresponding to residues in the PHF6 peptide are less affected, but their intensities in the sT_2R complex are also weaker than in the complex with T_2R (Figure S4, Table S2, Supporting Information).

It has been noted that the Tau−microtubule interaction varies according to the ionic strength.[8,50] In agreement with this, when repeating the NMR experiments with the same equimolar sample of TauF4 and the sT_2R complex in a higher PIPES concentration, we observed an intermediate position for many resonances of TauF4 (Figure 4). Assuming that the positions of the resonances in the spectrum of the 15 mM PIPES TauF4:sT_2R sample, with its 0.1 μM dissociation constant (Figure 3), represent the final fully saturated state, we derive a lower bound of 10 μM for the dissociation constant in 80 mM PIPES. This K_D value predicts a rapid exchange on the NMR time scale and hence a gradual shift of the resonances between free and bound state when the ratio of TauF4 to sT_2R is varied. This is what we observed for different titration points, which allowed us to assign a number of the weak resonances that we had only tentatively assigned on the basis of their proximity to their parent resonance. Thus, markers for the IR1/2 repeat region such as Ile277, Asn279, Leu282, and Ser285, be it with a very low intensity for the former two, could be assigned (Figure 4). In R2, Lys294 was identified as the peak with the most pronounced downfield proton chemical shift (Figure 4). For residues in the R1 repeat, however, intensity in the first point of the titration series was already at the limit of detection, confirming our previous observation that its resonances are completely broadened beyond detection in the spectrum of TauF4:T_2R

In conclusion, both the acidic tubulin C-terminal tails and the general electronegative surface of tubulin are major contributors to the tight interaction between TauF4 and the tubulin surface, and the tubulin tails contribute positively to the dynamical character of Tau in the T_2R complex.

TauF4 Binds to a Single Tubulin Heterodimer, with an Overhanging Peptide in the First MTBR. Whereas the above results concern the binding of TauF4 to a construct with two curved tubulin heterodimers, we attempted to learn more about an even earlier event, that would be its association with a first single tubulin heterodimer. For this, we used the stathmin-like domain designed to sequester a single tubulin heterodimer (this complex is named TR).[30] The 20 nM TauF4:TR tubulin dissociation constant derived from a FRET measurement (Figure 3) underscores the importance of the number of tubulin units for the interaction strength but should still lead to a stable complex on the NMR time scale. Because addition of more than 0.3 equiv of TauF4 to TR invariably led to precipitation of the sample at the concentrations required for NMR analysis, we recorded a TROSY spectrum with 0.3 equiv of TauF4.

When comparing the spectra of TauF4 in complex with TR or with T_2R, many resonances are very close in intensity and position, indicating a similar environment for many residues of TauF4 in complex with an assembly containing a single or two tubulin heterodimers. Nevertheless, we did observe two notable differences between both spectra. First, the resonances corresponding to the previously invisible R1 peptide in the TauF4:T_2R spectrum are now visible in the TauF4:TR spectrum, with easily detectable intensity for the ^{262}STEN^{265} tetrapeptide (Figure 5). Second, by contrast, the intensity of resonances corresponding to residues in the C-terminal part of TauF4, including the PHF6 peptide,[26] is much weaker when TauF4 is in complex with TR than in its complex with T_2R, and this despite the halving of the molecular weight of the TR versus T_2R complex (e.g., Tyr310 in Figure 5).

We previously observed that TauF4 binds less tightly to T_2R than to microtubules,[28] and our results indicate that some parts of the fragment retain significant mobility when associated with T_2R. The number and the conformation of the tubulin heterodimers that compose the surface available to TauF4 might be at the origin of these observations, but another possible explanation for the different behavior according to the tubulin assembly considered is that $RB3_{SLD}$ interferes with the binding of TauF4 to tubulin in T_2R, hence lowering the strength of interaction. To address this question, we turned to a second construct with a single tubulin heterodimer in which most of the stathmin-like domain is absent but for which assembly is prevented by a covalently linked peptide derived from the stathmin N-terminus. The resulting construct is named Ncap-tubulin.[33] In T_2R, the peptide of $RB3_{SLD}$ corresponding to the stathmin N-terminus interacts with the surface of α-tubulin engaged in longitudinal interactions when tubulin heterodimers are embedded in a microtubule.[29,51] Therefore, this surface is very unlikely to be involved in Tau binding. The peptide hence prevents the tubulin longitudinal associations but leaves the other surfaces of tubulin fully accessible. Because Ncap-tubulin contains only one tubulin heterodimer (as compared to two heterodimers in T_2R), for easier assessment of the effect of the stathmin-like domains on TauF4 binding, we compare the spectra of the TauF4:Ncap-tubulin complex with those of TauF4:TR. The $RB3_{SLD}$ C-terminal helix, that contacts both tubulin heterodimers of T_2R in a region that corresponds to the exterior of the microtubule,[41] is shortened in this complex but still occupies the same position relative to the tubulin heterodimer. The spectra

of TauF4 in the presence of both complexes (Ncap-tubulin and TR) are similar, with visible resonances of the overhanging peptide in the R1 repeat accompanied by a similar intensity reduction for the resonances of the PHF6 peptide residues in both spectra (Figure 5). This suggests that the C-terminal helix of the stathmin-like domain does not interfere significantly with the TauF4:tubulin interaction. The Asn265 resonance shifts slightly more in the TauF4:Ncap-tubulin complex than in the TauF4:TR complex. Although we cannot fully exclude a proximity of this residue to the $RB3_{SLD}$ helix that distinguishes both single tubulin heterodimer complexes, this differential shift can also reflect a proximity to the different Ncap peptides in these two constructs.

Our results with the single tubulin heterodimer hence suggest that the N- and C-terminal parts of TauF4 bind to a single tubulin heterodimer with an overhanging peptide in the first MTBR. Binding to a single tubulin heterodimer further leads to a lesser degree of mobility for the C-terminal part of the Tau fragment than when TauF4 binds to a construct with two tubulin heterodimers.

To identify any stable structure in this overhanging peptide in the TauF4:single tubulin complexes, we synthesized a peptide (residues 256 to 273 of Tau) centered on the residues that have observable intensities in the TauF4:TR complex spectrum but disappearing signals in that of TauF4:T_2R. The NOE spectrum of the peptide in a 40:1 ratio over T_2R shows that the positive Hα-H_N NOE characterizing the flexible Gly_{272}-Gly_{273} C-terminus in the free peptide becomes negative in the presence of T_2R, confirming both the interaction and the rapid exchange required for transfer-NOE[52] (Figure S5, Supporting Information). A number of sequential NOEs also gain substantially in intensity, and new contact NOEs notably between the amide protons of Ile_{260}-Gly_{261} and Asn_{265}-Leu_{266} could be detected even at a mixing time as low as 100 ms (Figure 6). As this suggests at least a partial structuring of this peptide at the tubulin surface, we searched in the PDB for sequence motif homologues to this peptide and identified an IGSTENI motif in the citrate synthase from *Francisella tularensis* (PDB code 3MSU), almost identical to the ^{260}IGSTENL^{266} central sequence of the Tau peptide. In the citrate synthase structure, this motif adopts a turn conformation, similarly characterized by short distances between the amide protons corresponding to those identified by NOE in the Tau peptide:T_2R complex.

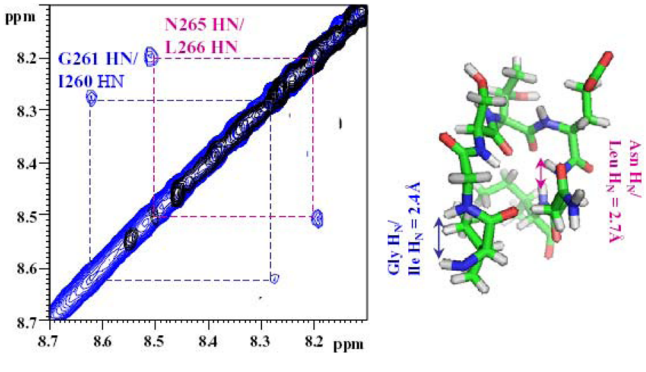

Figure 6. The conformation of the R1 repeat in its complex with T_2R. (Left) Homonuclear transfer-NOE spectrum on the VKSKIGSTENLKHQPGGG peptide of the Tau R1 repeat alone (black) or in the presence of 1:40 T_2R (blue). Additional cross-peaks stem from the bound conformation of the peptide. (Right) Loop region of the (E)IGSTEN(I) peptide in the citrate synthase crystal structure (PDB code 3MSU), with short distances between the Ile/Gly and And/Ile amide protons.

Altogether, the spectra of TauF4 with a single tubulin heterodimer show that N- and C-termini of TauF4 bind to a single tubulin heterodimer and hence suggest the presence of a turn between those fragments located in the first repeat. This turn, centered on the ^{260}IGSTENL^{266} peptide, thereby would not directly contact the single tubulin heterodimer. The C-terminus of TauF4 in this single tubulin heterodimer complex has partly lost the mobility it had in the T_2R complex with the two tubulin dimers.

TauF4 Binds Asymmetrically to the Two Tubulin Heterodimers in T_2R. The NMR spectra of TauF4 in the presence of assemblies comprising one or two tubulin heterodimers suggest that a protruding R1 MTBR peptide contacts the second tubulin heterodimer in T_2R but sticks out in the single tubulin heterodimer complexes. This scheme predicts that TauF4 would lose the interaction of this R1 MTBR peptide in the latter, and hence the affinities of TauF4 for TR or T_2R would differ, in agreement with our titration results (Figure 3).

We sought to further localize the TauF4 fragment on the T_2R surface by introducing four cysteine mutations in the $RB3_{SLD}$ helix, one in front of every tubulin subunit (Figure 7), and labeled them with a spin label to perform paramagnetic relaxation enhancement (PRE) experiments.[53,54] We then measured the spectra of TauF4 in the presence of these four

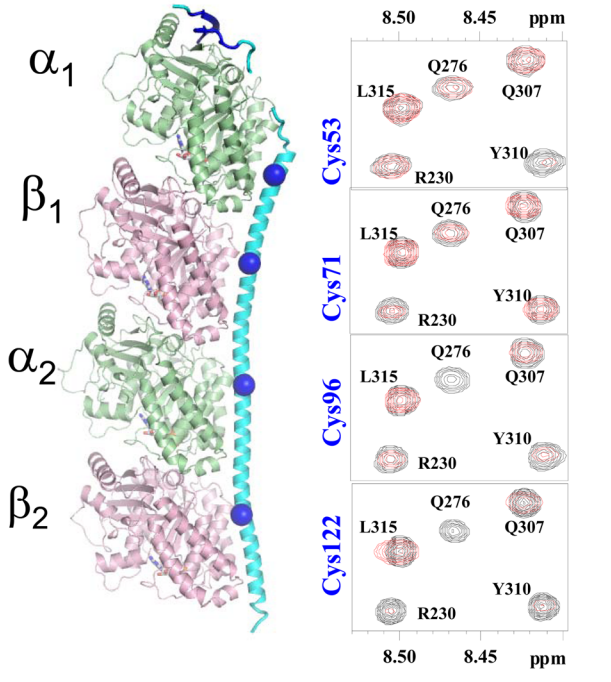

Figure 7. Positioning of TauF4 on the T_2R surface through the use of engineered spin labels in the $RB3_{SLD}$ helix. (Left) X-ray structure of T_2R (PDB code 3RYC). The Cαs of the $RB3_{SLD}$ residues mutated in cysteine for nitroxide labeling are shown as blue spheres. The residues corresponding to the stathmin-derived Ncap peptide are also highlighted in blue. The $RB3_{SLD}$ region that connects its N-terminal part to the C-terminal helix is disordered in the structure and not traced in this panel. (Right) Representative panels of the spectra of TauF4 in its complex with each of the four differently labeled T_2R complexes, in the absence (red) or presence (black) of vitamin C.

dx.doi.org/10.1021/ja504864m | J. Am. Chem. Soc. 2014, 136, 12615−12623

different T_2R complexes, each one with a single label on $RB3_{SLD}$ to detect possible spatial proximity at a per-residue level. In agreement with the low-contrast detected by cryoelectron microscopy of Tau-decorated microtubules,[10] all spin labels had some effect on most of the resonances. Nevertheless, the most pronounced signal disappearance for many TauF4 resonances was observed when the spin label was attached to Cys122, in front of the β2 subunit, with for example a vanishing intensity for the resonances of Arg230 in the PRR (Figure 7) and Ser241 and Leu243 at the hinge between the PRR and first MTBR (Figure S6, Supporting Information). The spin label at Cys71, in front of β1, had a less pronounced effect and quenched the intensity of the same resonances only to a level of 60%. The PRR is therefore predominantly positioned in the vicinity of the β2 subunit, indicating an asymmetrical contribution of the two tubulin heterodimers of T_2R in their role toward TauF4 binding. We further observed an almost complete extinction of the resonances of the PHF6 ^{309}VYK^{311} residues, close to the C-terminal end of TauF4, when the spin label was in front of this β2 tubulin subunit (Figure 7). This agrees with an overall structure of TauF4 bound to the α2/β2 tubulin heterodimer in T_2R with a turn-like character.

Most surprisingly, however, the spin label at Cys53, in front of α1, weakens these selected resonances to the same extent of the PHF6 peptide (Figures 7 and S6, Supporting Information). In the structure of T_2R, the distance between the Cαs of the corresponding labeled residues of $RB3_{SLD}$ (residues 53 and 122, in front of α1 and β2, respectively) is larger than 100 Å, whereas the expected sphere of activity of the spin label has been estimated to be 20 to 25 Å.[55] Therefore, even when taking into account the size of the spin label itself, mostly 8 to 10 Å away from the main chain atoms, the spheres of activity in T_2R of $RB3_{SLD}$ labeled at position 53 and 122 do not overlap. Whereas an intensity decrease of these PHF6 resonances by the spin label at Cys71, in front of β1 and hence equivalent to the Cys122 position in front of β2, could have pointed to the existence of similar binding modes of TauF4 to both tubulin heterodimers, we interpret the PRE data with the spin label at Cys53 as evidence for the mobility of the C-terminal moiety of TauF4 between two distal positions located at either T_2R end.

DISCUSSION

Past attempts to elucidate the details of how Tau interacts with tubulin have revealed the crucial role of the PRR and MTBR regions in the interaction with stabilized MTs and in promotion of tubulin assembly.[6,4,8,28] We previously defined the TauF4 fragment that spans this central region and functionally mimics full length Tau for microtubule assembly. The tighter binding of TauF4 to straight microtubular tubulin can provide the driving force to straighten the soluble curved tubulin heterodimers, the conformation found in T_2R, and thereby promote polymerization. However, a view of how this central region of Tau behaves when in complex with any form of tubulin surface has been missing. Here we present NMR data on the interaction of TauF4 with several soluble constructs containing a single or two tubulin heterodimers in their curved conformation. These constructs do not recapitulate a possible role of Tau in establishing lateral contacts between the protofilaments, but the corresponding complexes should represent the early intermediates in the assembly of tubulin heterodimers into MTs by Tau.

TauF4 binds to one tubulin heterodimer with a sizable affinity (Figure 3). We propose it does so in a U-turn manner (Figure 8). In the complex, the IR2/3 region has a reduced mobility, as witnessed by the low intensities for these residues in the TauF4-TR spectra (Figure 5). This argues against this region playing a "fly-casting" role to recruit a second tubulin heterodimer.[56] In TauF4-TR, an overhanging peptide in the first Tau MTBR (R1) maintains sufficient mobility in the complex to be visible in the NMR spectrum (Figure 5). Only when a second tubulin heterodimer comes in, as mimicked by the T_2R complex, does this peptide become immobilized. Together with the increased GTP hydrolysis rate of the tubulin–colchicine complex upon addition of TauF4 and TauF4's capacity to promote the oligomerization of tubulin heterodimers into ring-like structures (Figure 2), these data point to a role for TauF4 in longitudinal tubulin assembly through recruitment of a second tubulin heterodimer by the first repeat of TauF4 (Figure 8). This R1 region spans the "assembly-promoting" peptide sequence that was early on identified to promote MT assembly, albeit at a 100-fold higher concentration than that of full-length Tau.[57]

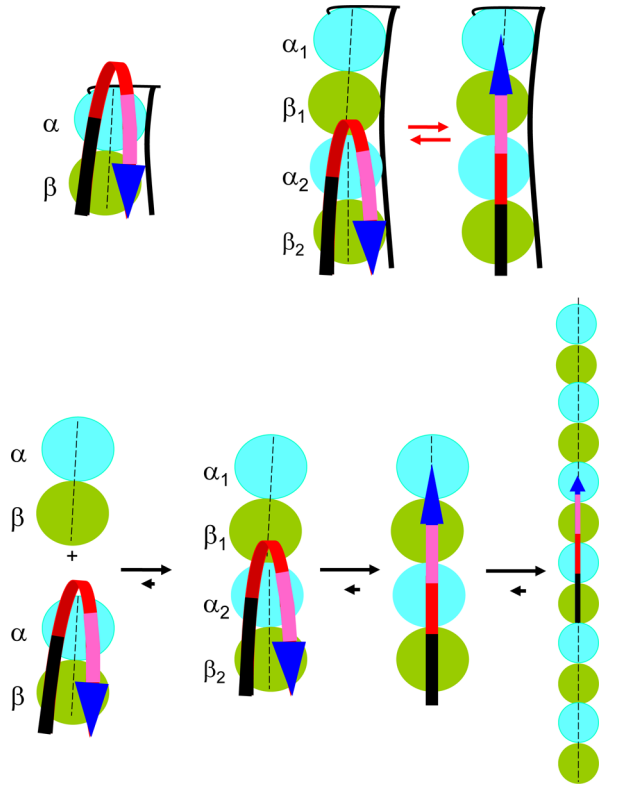

Figure 8. Model for the interaction of TauF4 with tubulin heterodimers, in the presence (top) or absence (bottom) of $RB3_{SLD}$. The regions of TauF4 are colored according to Figure 1. In the TR complex (top, left), TauF4 binds in a U-turn conformation, whereby the IGSTEN peptide protrudes from the tubulin surface and can hook on a second tubulin. This is modeled by the T_2R complex (top, right), in which the C-terminus of TauF4 now gains in mobility, translating in the experimentally observed swing movement of the PHF6 peptide. In the absence of the SLD domain, TauF4 favors tubulin longitudinal associations leading to enhanced GTPase activity of the tubulin–colchicine complex (bottom, middle) and to the assembly into protofilaments forming rings at 20 °C (Figure 2) or MTs when incubated at 37 °C (bottom, right). The model should not be taken as a static picture of TauF4, in view of the important mobility of this Tau fragment on the tubulin surface.

dx.doi.org/10.1021/ja504864m | J. Am. Chem. Soc. 2014, 136, 12615–12623

At the other end of the microtubule assembly−disassembly cycle, during shrinkage, tubulin heterodimers become curved when protofilaments are peeling off;[58] hence, their interaction with Tau may become more similar to what we observe in the case of T_2R. Such a complex is characterized by an increased mobility of the C-terminal part of TauF4, most dramatically illustrated by the movement of the PHF6 peptide, whose resonances are affected by spin labels in the vicinity of both the α1 and the β2 subunits in T_2R. Tubulin heterodimer dissociation could be slowed down by the overhanging R1 region of Tau and, additionally, by the swing movement of the IR2/3 region that keeps two curved tubulin heterodimers connected (Figure 8). Altogether, such a model also explains the prevention of catastrophes by Tau.[3,4]

The downfield shifts of many of the $^{1}H-^{15}N$ correlations in our TauF4:tubulin complexes, even without its C-terminal acidic tails (Figure 4), together with the steep salt dependence of the interaction, suggest that a general electrostatic interaction is one of the major driving forces for the interaction of Tau with tubulin. This is also consistent with the high flexibility of TauF4 in its complex with T_2R and the apparent absence of a single binding pocket on the tubulin surface. Less well characterized than an interaction model whereby specific van der Waals interactions, hydrogen bonds, or ionic bonds provide the free energy of binding, the Tau:tubulin interaction is distinguished from that of many other IUPs that bind to their target molecule in a well-defined conformation.[23]

Few additional cases have been described where an IUP remains mobile upon binding to its target. One example is the complex of the cyclin-dependent kinase inhibitor Sic1 with the F-box protein Cdc4, where several phosphorylated motifs target a similar binding pocket in a highly dynamical manner.[59] The binding of Sic1 is conditioned by a minimal number of phosphorylation events.[60] For Tau, phosphorylation is not required for interaction with tubulin. Rather, the different phosphorylation patterns that define its physiological but also pathologically aggregated state[61] would regulate its interaction with and its assembly capacity of tubulin in an as yet poorly understood manner. The major proton chemical shift observed for Leu215, directly neighboring Ser214 that upon phosphorylation leads to a strongly decreased affinity of Tau for the MT surface,[62,63] suggests that specific phosphorylation events can interfere with interaction hotspots. Similarly, Ser262, which upon phosphorylation by the Mark kinase was reported to lead to detachment of Tau from the MTs,[64,65] is at the very center of the "invisible" region of TauF4 in its complex with T_2R. Our experimental approach based on NMR analysis of soluble tubulin constructs with a Tau fragment, together with our capacity to generate in vitro well-defined phosphorylation patterns,[66] will allow us to study the regulation of Tau by phosphorylation in an unprecedented manner.

CONCLUSION

We present experimental evidence that a functional fragment of Tau, TauF4, promotes the longitudinal interaction between tubulin heterodimers. Using NMR spectroscopy of TauF4 in complex with different soluble tubulin heterodimer structures, we present a model that can explain how TauF4 promotes the assembly of microtubules from tubulin heterodimers.

ASSOCIATED CONTENT

Supporting Information

Supplemental Figures S1−6. Supplemental Tables T1−T3. Preparation of SLD-based tubulin complexes. Analysis of the interaction of TauF4 with complexes of tubulin and stathmin-like-based proteins. Effect of TauF4 on the tubulin−colchicine GTPase activity. Tubulin ring formation by TauF4. Preparation of TauF4 samples for NMR spectroscopy. NMR spectroscopy. This material is available free of charge via the Internet at http://pubs.acs.org.

AUTHOR INFORMATION

Corresponding Author

Guy.Lippens@univ-lille1.fr

Author Contributions

[+]B.G. and I.L. contributed equally to this work.

Notes

The authors declare no competing financial interest.

ACKNOWLEDGMENTS

We thank Dr. C. Byrne (Paris, France) for careful reading of the paper, Drs. B. Fritzinger and F.-X. Cantrelle for excellent maintenance of the NMR spectrometers and Mr. D. Mauchand (Unité Commune d'Expérimentation Animale, Institut National de la Recherche Agronomique) for providing us with the material from which tubulin was purified. We gratefully acknowledge access to the mass spectrometry facilities of the Laboratoire de Spectrométrie de Masse (Institut de Chimie des Substances Naturelles, Gif-sur-Yvette) and Vincent Guérineau from this laboratory for advice during MS data recording. The research leading to these results was supported by the Centre National de la Recherche Scientifique, the Agence Nationale de la Recherche (ANR-05-Blanc-6320-01, ANR-12-BSV8-0002-01, and program MALZ-TAF), the LABEX (laboratory of excellence program investment for the future) DISTALZ grant (Development of Innovative Strategies for a Transdisciplinary approach to ALzheimer's disease), the Fondation ARC pour le Recherche sur le Cancer, and the CNRS Large Scale Facility NMR THC Fr3050. The NMR facility is funded by the European Community, the CNRS, the Région Nord-Pas de Calais (France), the University of Lille 1, and the Institut Pasteur de Lille.

DEDICATION

[⊥]We dedicate this paper to the memory of Dr. Jean-Michel Wieruszeski, who untimely passed away during this study.

REFERENCES

(1) Cleveland, D. W.; Hwo, S. Y.; Kirschner, M. W. *J. Mol. Biol.* **1977**, *116*, 207−225.
(2) Drubin, D. G.; Kirschner, M. W. *J. Cell Biol.* **1986**, *103*, 2739−2746.
(3) Murphy, D. B.; Johnson, K. A.; Borisy, G. G. *J. Mol. Biol.* **1977**, *117*, 33−52.
(4) Trinczek, B.; Biernat, J.; Baumann, K.; Mandelkow, E. M.; Mandelkow, E. *Mol. Biol. Cell* **1995**, *6*, 1887−1902.
(5) Butner, K. A.; Kirschner, M. W. *J. Cell Biol.* **1991**, *115*, 717−730.
(6) Gustke, N.; Trinczek, B.; Biernat, J.; Mandelkow, E. M.; Mandelkow, E. *Biochemistry* **1994**, *33*, 9511−9522.
(7) Goode, B. L.; Feinstein, S. C. *J. Cell Biol.* **1994**, *124*, 769−782.
(8) Goode, B. L.; Denis, P. E.; Panda, D.; Radeke, M. J.; Miller, H. P.; Wilson, L.; Feinstein, S. C. *Mol. Biol. Cell* **1997**, *8*, 353−365.

(9) Al-Bassam, J.; Ozer, R. S.; Safer, D.; Halpain, S.; Milligan, R. A. *J. Cell Biol.* **2002**, *157*, 1187−1196.
(10) Santarella, R. A.; Skiniotis, G.; Goldie, K. N.; Tittmann, P.; Gross, H.; Mandelkow, E.-M.; Mandelkow, E.; Hoenger, A. *J. Mol. Biol.* **2004**, *339*, 539−553.
(11) Schaap, I. A. T.; Hoffmann, B.; Carrasco, C.; Merkel, R.; Schmidt, C. F. *J. Struct. Biol.* **2007**, *158*, 282−292.
(12) Tsvetkov, P. O.; Makarov, A. A.; Malesinski, S.; Peyrot, V.; Devred, F. *Biochimie* **2012**, *94*, 916−919.
(13) Makrides, V.; Massie, M. R.; Feinstein, S. C.; Lew, J. *Proc. Natl. Acad. Sci. U. S. A.* **2004**, *101*, 6746−6751.
(14) Kar, S.; Fan, J.; Smith, M. J.; Goedert, M.; Amos, L. A. *EMBO J.* **2003**, *22*, 70−77.
(15) Prota, A. E.; Bargsten, K.; Zurwerra, D.; Field, J. J.; Díaz, J. F.; Altmann, K.-H.; Steinmetz, M. O. *Science* **2013**, *339*, 587−590.
(16) Choi, M. C.; Raviv, U.; Miller, H. P.; Gaylord, M. R.; Kiris, E.; Ventimiglia, D.; Needleman, D. J.; Kim, M. W.; Wilson, L.; Feinstein, S. C.; Safinya, C. R. *Biophys. J.* **2009**, *97*, 519−527.
(17) Hinrichs, M. H.; Jalal, A.; Brenner, B.; Mandelkow, E.; Kumar, S.; Scholz, T. *J. Biol. Chem.* **2012**, *287*, 38559−38568.
(18) Cleveland, D. W.; Hwo, S. Y.; Kirschner, M. W. *J. Mol. Biol.* **1977**, *116*, 227−247.
(19) Schweers, O.; Schönbrunn-Hanebeck, E.; Marx, A.; Mandelkow, E. *J. Biol. Chem.* **1994**, *269*, 24290−24297.
(20) Mukrasch, M. D.; Biernat, J.; von Bergen, M.; Griesinger, C.; Mandelkow, E.; Zweckstetter, M. *J. Biol. Chem.* **2005**, *280*, 24978−24986.
(21) Smet, C.; Leroy, A.; Sillen, A.; Wieruszeski, J.-M.; Landrieu, I.; Lippens, G. *ChemBioChem* **2004**, *5*, 1639−1646.
(22) Eliezer, D.; Barré, P.; Kobaslija, M.; Chan, D.; Li, X.; Heend, L. *Biochemistry* **2005**, *44*, 1026−1036.
(23) Janin, J.; Sternberg, M. J. E. *F1000 Biol. Rep.* **2013**, *5* (2), doi: 10.3410/B5-2.
(24) Lee, G.; Cowan, N.; Kirschner, M. *Science* **1988**, *239*, 285−288.
(25) Lee, G.; Neve, R. L.; Kosik, K. S. *Neuron* **1989**, *2*, 1615−1624.
(26) Von Bergen, M.; Friedhoff, P.; Biernat, J.; Heberle, J.; Mandelkow, E. M.; Mandelkow, E. *Proc. Natl. Acad. Sci. U. S. A.* **2000**, *97*, 5129−5134.
(27) Von Bergen, M.; Barghorn, S.; Li, L.; Marx, A.; Biernat, J.; Mandelkow, E. M.; Mandelkow, E. *J. Biol. Chem.* **2001**, *276*, 48165−48174.
(28) Fauquant, C.; Redeker, V.; Landrieu, I.; Wieruszeski, J.-M.; Verdegem, D.; Laprévote, O.; Lippens, G.; Gigant, B.; Knossow, M. *J. Biol. Chem.* **2011**, *286*, 33358−33368.
(29) Ravelli, R. B. G.; Gigant, B.; Curmi, P. A.; Jourdain, I.; Lachkar, S.; Sobel, A.; Knossow, M. *Nature* **2004**, *428*, 198−202.
(30) Mignot, I.; Pecqueur, L.; Dorléans, A.; Karuppasamy, M.; Ravelli, R. B. G.; Dreier, B.; Plückthun, A.; Knossow, M.; Gigant, B. *J. Biol. Chem.* **2012**, *287*, 31085−31094.
(31) Dorleans, A.; Knossow, M.; Gigant, B. *Methods Mol. Med.* **2007**, *137*, 235−243.
(32) Nawrotek, A.; Knossow, M.; Gigant, B. *J. Mol. Biol.* **2011**, *412*, 35−42.
(33) Wang, W.; Jiang, Q.; Argentini, M.; Cornu, D.; Gigant, B.; Knossow, M.; Wang, C. *J. Biol. Chem.* **2012**, *287*, 15143−15153.
(34) Heusèle, C.; Carlier, M. F. *Biochem. Biophys. Res. Commun.* **1981**, *103*, 332−338.
(35) Wang, C.; Cormier, A.; Gigant, B.; Knossow, M. *Biochemistry* **2007**, *46*, 10595−10602.
(36) Gigant, B.; Wang, C.; Ravelli, R. B. G.; Roussi, F.; Steinmetz, M. O.; Curmi, P. A.; Sobel, A.; Knossow, M. *Nature* **2005**, *435*, 519−522.
(37) Devred, F.; Barbier, P.; Douillard, S.; Monasterio, O.; Andreu, J. M.; Peyrot, V. *Biochemistry* **2004**, *43*, 10520−10531.
(38) Christodoulou, J.; Larsson, G.; Fucini, P.; Connell, S. R.; Pertinhez, T. A.; Hanson, C. L.; Redfield, C.; Nierhaus, K. H.; Robinson, C. V.; Schleucher, J.; Dobson, C. M. *Proc. Natl. Acad. Sci. U. S. A.* **2004**, *101*, 10949−10954.
(39) Mukrasch, M. D.; von Bergen, M.; Biernat, J.; Fischer, D.; Griesinger, C.; Mandelkow, E.; Zweckstetter, M. *J. Biol. Chem.* **2007**, *282*, 12230−12239.
(40) Sillen, A.; Barbier, P.; Landrieu, I.; Lefebvre, S.; Wieruszeski, J.-M.; Leroy, A.; Peyrot, V.; Lippens, G. *Biochemistry* **2007**, *46*, 3055−3064.
(41) Gigant, B.; Curmi, P. A.; Martin-Barbey, C.; Charbaut, E.; Lachkar, S.; Lebeau, L.; Siavoshian, S.; Sobel, A.; Knossow, M. *Cell* **2000**, *102*, 809−816.
(42) Sibille, N.; Huvent, I.; Fauquant, C.; Verdegem, D.; Amniai, L.; Leroy, A.; Wieruszeski, J.-M.; Lippens, G.; Landrieu, I. *Proteins Struct. Funct. Bioinf.* **2012**, *80*, 454−462.
(43) Sibille, N.; Sillen, A.; Leroy, A.; Wieruszeski, J.-M.; Mulloy, B.; Landrieu, I.; Lippens, G. *Biochemistry* **2006**, *45*, 12560−12572.
(44) Andronesi, O. C.; von Bergen, M.; Biernat, J.; Seidel, K.; Griesinger, C.; Mandelkow, E.; Baldus, M. *J. Am. Chem. Soc.* **2008**, *130*, 5922−5928.
(45) Sawaya, M. R.; Sambashivan, S.; Nelson, R.; Ivanova, M. I.; Sievers, S. A.; Apostol, M. I.; Thompson, M. J.; Balbirnie, M.; Wiltzius, J. J. W.; McFarlane, H. T.; Madsen, A. Ø.; Riekel, C.; Eisenberg, D. *Nature* **2007**, *447*, 453−457.
(46) Serrano, L.; Montejo de Garcini, E.; Hernández, M. A.; Avila, J. *Eur. J. Biochem.* **1985**, *153*, 595−600.
(47) Littauer, U. Z.; Giveon, D.; Thierauf, M.; Ginzburg, I.; Ponstingl, H. *Proc. Natl. Acad. Sci. U. S. A.* **1986**, *83*, 7162−7166.
(48) Prota, A. E.; Magiera, M. M.; Kuijpers, M.; Bargsten, K.; Frey, D.; Wieser, M.; Jaussi, R.; Hoogenraad, C. C.; Kammerer, R. A.; Janke, C.; Steinmetz, M. O. *J. Cell Biol.* **2013**, *200*, 259−270.
(49) Moon, S.; Case, D. A. *J. Biomol. NMR* **2007**, *38*, 139−150.
(50) Duan, A. R.; Goodson, H. V. *Mol. Biol. Cell* **2012**, *23*, 4796−4806.
(51) Clément, M.-J.; Jourdain, I.; Lachkar, S.; Savarin, P.; Gigant, B.; Knossow, M.; Toma, F.; Sobel, A.; Curmi, P. A. *Biochemistry* **2005**, *44*, 14616−14625.
(52) Lippens, G.; Hallenga, K.; Van Belle, D.; Wodak, S. J.; Nirmala, N. R.; Hill, P.; Russell, K. C.; Smith, D. D.; Hruby, V. J. *Biochemistry* **1993**, *32*, 9423−9434.
(53) Kosen, P. A. *Methods Enzymol.* **1989**, *177*, 86−121.
(54) Battiste, J. L.; Wagner, G. *Biochemistry* **2000**, *39*, 5355−5365.
(55) Gillespie, J. R.; Shortle, D. *J. Mol. Biol.* **1997**, *268*, 170−184.
(56) Shoemaker, B. A.; Portman, J. J.; Wolynes, P. G. *Proc. Natl. Acad. Sci. U. S. A.* **2000**, *97*, 8868−8873.
(57) Aizawa, H.; Kawasaki, H.; Murofushi, H.; Kotani, S.; Suzuki, K.; Sakai, H. *J. Biol. Chem.* **1989**, *264*, 5885−5890.
(58) Chrétien, D.; Fuller, S. D.; Karsenti, E. *J. Cell Biol.* **1995**, *129*, 1311−1328.
(59) Tang, X.; Orlicky, S.; Mittag, T.; Csizmok, V.; Pawson, T.; Forman-Kay, J. D.; Sicheri, F.; Tyers, M. *Proc. Natl. Acad. Sci. U. S. A.* **2012**, *109*, 3287−3292.
(60) Nash, P.; Tang, X.; Orlicky, S.; Chen, Q.; Gertler, F. B.; Mendenhall, M. D.; Sicheri, F.; Pawson, T.; Tyers, M. *Nature* **2001**, *414*, 514−521.
(61) Hasegawa, M.; Morishima-Kawashima, M.; Takio, K.; Suzuki, M.; Titani, K.; Ihara, Y. *J. Biol. Chem.* **1992**, *267*, 17047−17054.
(62) Zheng-Fischhöfer, Q.; Biernat, J.; Mandelkow, E. M.; Illenberger, S.; Godemann, R.; Mandelkow, E. *Eur. J. Biochem.* **1998**, *252*, 542−552.
(63) Landrieu, I.; Lacosse, L.; Leroy, A.; Wieruszeski, J.-M.; Trivelli, X.; Sillen, A.; Sibille, N.; Schwalbe, H.; Saxena, K.; Langer, T.; Lippens, G. *J. Am. Chem. Soc.* **2006**, *128*, 3575−3583.
(64) Biernat, J.; Gustke, N.; Drewes, G.; Mandelkow, E. M.; Mandelkow, E. *Neuron* **1993**, *11*, 153−163.
(65) Drewes, G.; Ebneth, A.; Preuss, U.; Mandelkow, E. M.; Mandelkow, E. *Cell* **1997**, *89*, 297−308.
(66) Lippens, G.; Amniai, L.; Wieruszeski, J.-M.; Sillen, A.; Leroy, A.; Landrieu, I. *Biochem. Soc. Trans.* **2012**, *40*, 698−703.